CORROSION SCIENCE AND TECHNOLOGY, Vol.20, No.1(2021), pp.26~36
[Research Paper]
pISSN: 1598-6462 / eISSN: 2288-6524
DOI: https://doi.org/10.14773/cst.2021.20.1.26

Ultrasonic Cavitation Behavior and its Degradation Mechanism of Epoxy Coatings in 3.5 % NaCl at 15 °C

I. J. Jang, J. M. Jeon, K. T. Kim, Y. R. Yoo, and Y. S. Kim†

Materials Research Centre for Energy and Clean Technology,
School of Materials Science and Engineering, Andong National University,
1375 Gyeongdong-ro, Andong, Gyeongbuk, 36729, Korea

(Received February 09, 2021; Revised February 24, 2021; Accepted February 24, 2021)

Pipes operating in the seawater environment faces cavitation degradation and corrosion of the metallic component, as well as a negative synergistic effect. Cavitation degradation shows the mechanism by which materials deteriorate by causing rapid change of pressure or high-frequency vibration in the solution, and introducing the formation and explosion of bubbles. In order to rate the cavitation resistance of materials, constant conditions have been used. However, while a dynamic cavitation condition can be generated in a real system, there has been little reported on the effect of ultrasonic amplitude on the cavitation resistance and mechanism of composites. In this work, 3 kinds of epoxy coatings were used, and the cavitation resistance of the epoxy coatings was evaluated in 3.5% NaCl at 15 °C using an indirect ultrasonic cavitation method. Eleven kinds of mechanical properties were obtained, namely compressive strength, flexural strength and modulus, tensile strength and elongation, Shore D hardness, water absorptivity, impact test, wear test for coating only and pull-off strength for epoxy coating/carbon steel or epoxy coating/rubber/carbon steel. The cavitation erosion mechanism of epoxy coatings was discussed on the basis of the mechanical properties and the effect of ultrasonic amplitude on the degradation of coatings.

Keywords: *Ultrasonic Cavitation test, Amplitude, Epoxy coating, 3.5% NaCl*

1. Introduction

Pipes operating in the seawater environment faces cavitation degradation, corrosion of the metallic component, as well as a deleterious synergistic effect [1-4]. Cavitation degradation shows the mechanism by which materials deteriorate by the causing of rapid change of pressure or high-frequency vibration in the solution, and the introduction of the formation and explosion of bubbles. When the bubbles explode on the surface, micro-jets with high velocity and impact pressure including instantaneous high temperature can be formed [5,6] This impact energy and increased temperature induces cracking through plastic deformation and the propagation of cracks degrades the surface, causing erosion and corrosion [7-9].

Recently, we reported the effect of ultrasonic amplitude on the cavitation corrosion rate of 0.42 % C carbon steel in 3.5 % NaCl at 15 °C [10]; The corrosion rate of the specimen in the stagnant test solution was 0.02 mm/y, but in the case of 2 h cavitation corrosion test, the corrosion rate was 5.72 mm/y, and as the ultrasonic amplitude increased, the corrosion rate was greatly increased; at the ultrasonic amplitude 85 μm, the corrosion rate was abruptly increased to 21.63 mm/y.

Since the low corrosion resistance materials showed a very high corrosion rate, rubber lined steel pipes in a cavitation environment have been used for protection from seawater corrosion inside the pipeline. As the pipeline operates for a very long time over several tens of years, many cases of degradation have been reported, which have been caused by the aging of the lining materials, such as cavitation erosion in high flow velocity parts including the narrowed cross-sectional area of valves and orifices, slurry abrasion, and cracking due to the degradation of physical properties [11-14]. In order to enhance the performance of materials in a harsh and/or cavitation environment, several materials have been developed and evaluated; rubber [15,16], composites [17,18], metals [19], etc. Each composite material systems was usually evaluated using a modified ASTM G32 vibratory induced cavitation

†Corresponding author: yikim@anu.ac.kr
I. J. Jang: Master, J. M. Jeon: Master, K. T. Kim: Postdocs, Y. R. Yoo: Research Professor, Y. S. Kim: Professor

test method. This indirect cavitation method (in this work, called 'Practice B') in which the sample was held stationary at a distance under the oscillating horn tip, gives a variety of flexibility in evaluating both cored composites and soft elastomer materials, because of the differences in the cavitation energy imparted to the sample, and the size of the cavitation area [19]. In order to rate the cavitation resistance of materials, a constant conditions (ex. 20 kHz and a certain ultrasonic amplitude) have been used. However, while a dynamic cavitation condition can be generated in a real system, there have been few reports on the effect of ultrasonic amplitude on the cavitation resistance and erosion mechanism of composites.

In this work, three kinds of epoxy coatings were used and the cavitation resistance of the epoxy coatings was evaluated in 3.5% NaCl at 15 °C using an indirect cavitation method. The cavitation mechanism of epoxy coatings is discussed on the basis of mechanical properties and the effect of ultrasonic amplitude on the degradation of coatings.

2. Experimental Methods

2.1 Materials

Three kinds of epoxy coating were used, and each specimen was made by the respective supply company. In this work, 'A coating', 'B coating', and 'C coating' are designated, respectively. All specimens for cavitation test have 3 mm thickness and 29 mm diameter.

2.2 Mechanical test

Several mechanical tests for the three kinds of coatings were performed according to each standards as follows; compressive strength [20], flexural strength and modulus [21], tensile strength and elongation [22], Shore D hardness [23], water absorptivity [24], impact test [25], wear test [26] for coating only and pull-off strength for epoxy coating/carbon steel or epoxy coating/rubber/carbon steel [27].

2.3 Cavitation erosion test

2.3.1 Test equipment and test condition

The cavitation erosion tester (R&B-RB111-CE, Korea) was made by a magnetostrictive-driven method and by modifying ASTM G32 standard [10,28]; Maximum power output of the tester was 1,000 W, and an ultrasonic transducer showing (20 ± 5 KHz) was used. The horn tip was made by super duplex stainless steel (Fe-25.8Cr-2.3Mo -0.2W-0.5Si-10.7Ni-0.65Mn-0.03C-0.42N), and its diameter was 16 mm. The distance between the horn tip and

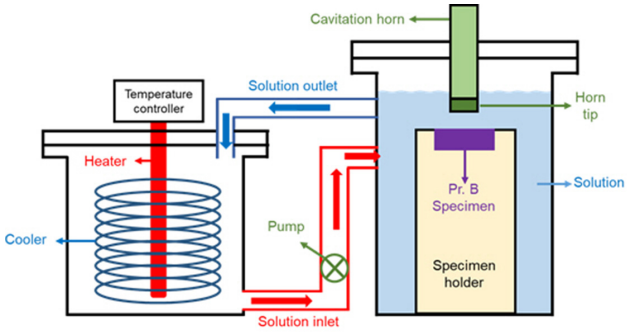

Fig. 1 Schematic of the cavitation erosion test equipment.

specimen was 0.5mm and a freshly ground (# 2,000 SiC) horn tip was used in every test. Fig. 1 shows a schematic of the cavitation erosion tester using an indirect cavitation method. Test specimen having a diameter of 29 mm was used as-fabricated, and after installing in a test cell, cavitation erosion tests were performed for 2, 4, and 6 h using an ultrasonic amplitude of 15, 50, and 85 μm (in this work, the peak-to-peak amplitude was termed 'ultrasonic amplitude'). The cavitation erosion rate was calculated on the basis of weight loss.

2.3.2 Surface analysis

Surface morphology was observed using a digital camera, 3D Stereographic microscopy (HIROX, KH-7700, Japan), FE-SEM (TESCAN, LYRA 3 XMH, Czech Republic) and EDS(TESCAN, VEGA II LMU, Czech Republic). The surface of the specimen for the analysis was coated with osmium.

3. Results and Discussion

3.1 Specimen and mechanical properties of epoxy coatings

This work used three kinds of coatings. Because each of the three kinds of specimens was made by different manufacturer, the specimen preparation procedure was different. Fig. 2 shows the surface appearance before cavitation erosion test of A coating, B coating, and C coating; Fig. 2a, b, c show the photos by digital camera, and A and B coating are ivory-colored, while C coating is green-colored. Fig. 2a', b', c' reveal the topography (magnification; ×35) on the surface of the A, B, and C coatings by 3D stereographic microscopy respectively. Every coating has a range of roughness, and the maximum depths of A, B, and C coatings were 110.7, 270.2 and 53.5 μm respectively. Fig. 2a", b", c" depict the SEM image of A, B, and C coatings respectively. Coatings were composed of the matrix and the compound. A and B coatings (magnification; ×500) had thin and flat com-

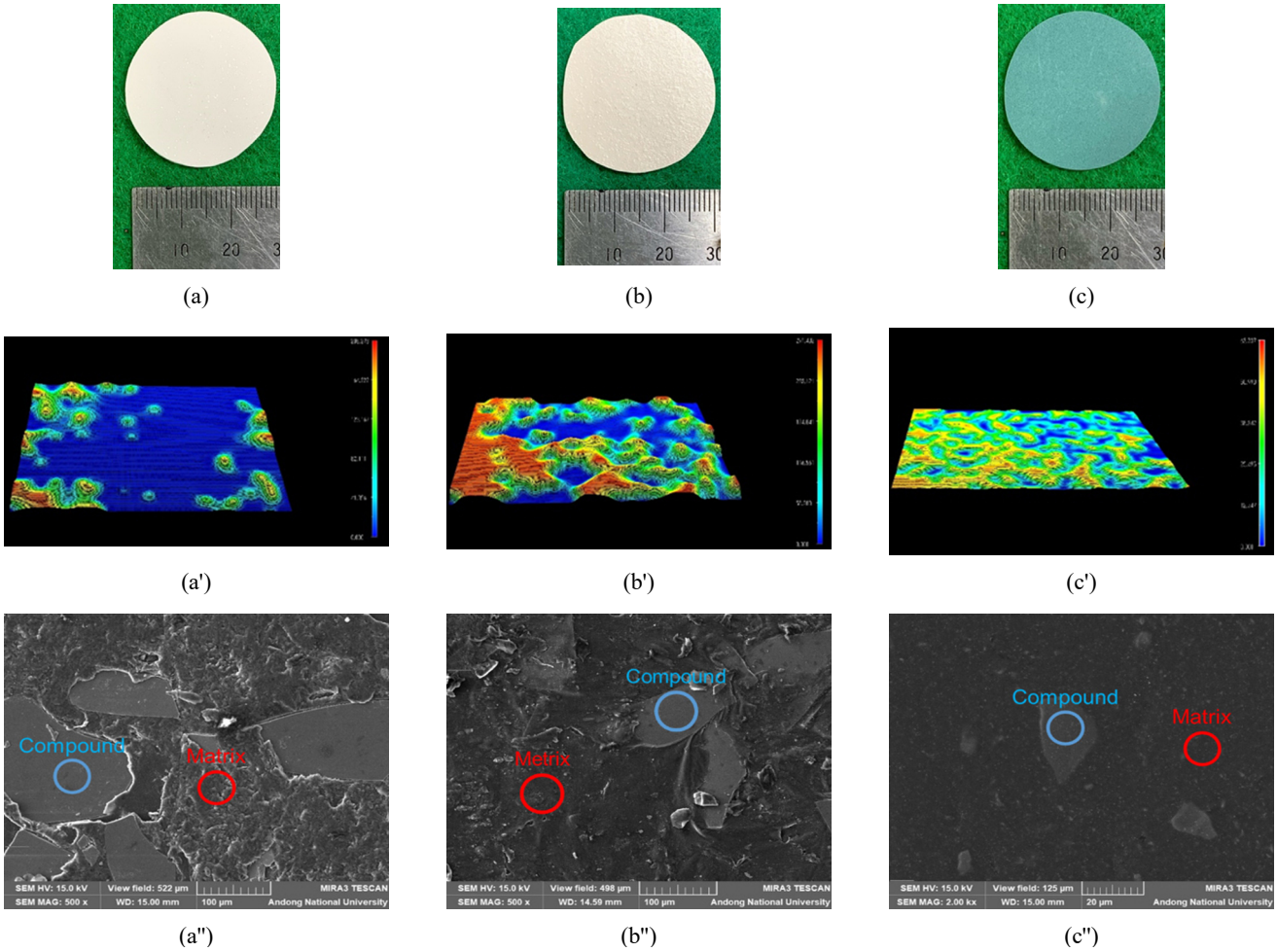

Fig. 2 Surface appearance before cavitation erosion test of (a, a', a") A coating, (b, b', b") B coating, (c, c', c") C coating; (a)(b)(c) Digital camera, (a')(b')(c') 3D Topography, (a")(b")(c") SEM image.

Table 1 Chemical composition of the three kinds of coating obtained from EDS analysis

Coatings	wt%	C	O	Si	Ti	Na	Mg	Al	K	Ca	Zn	Total
A	Matrix	26.6	72.02	0.52	0.86	-	-	-	-	-	-	100
	Compound	-	46.51	33.22	-	7.84	1.48	2.41	0.86	4.89	2.79	100
B	Matrix	26.51	72.03	0.91	0.55	-	-	-	-	-	-	100
	Compound	-	45.41	33.11	-	6.59	1.58	2.99	1.88	5.72	2.72	100
C	Matrix	26.78	72.26	0.57	0.39	-	-	-	-	-	-	100
	Compound	5.11	56.9	37.99	-	-	-	-	-	-	-	100

pounds, but C coating (magnification; ×2,000) showed a small and polygonal compound. Table 1 shows the chemical composition of the three kinds of coating obtained from EDS analysis. The matrices were the epoxy-base materials composed of carbon and oxygen, regardless of the A, B, and C coating. The compounds of A and B coatings were composed of oxygen and silicon, including several elements, such as Na and Ca. On the other hand, the compound of C coating was composed of oxygen and silicon and carbon etc. (The exact chemical composition could not be identified, because of each manufacturer's proprietary know-how).

Table 2 summarizes the mechanical properties of the three kinds of coating. Mechanical tests performed were

Table 2 Mechanical properties of the three kinds of coating

Property	Unit	A coating	B coating	C coating	Reference
Compressive strength	MPa	73.2	95.8	81.2	ASTM D695[20]
Flexural strength	MPa	35.6	59.4	94.1	ASTM D790[21]
Flexural modulus	GPa	5.29	5.02	5.13	
Tensile strength	MPa	15.3	30.8	59.2	ASTM D638[22]
Tensile elongation	%	0.34	0.71	1.61	
Shore D hardness	D	88	82	88	ASTM D2240[23]
Water absorptivity	$g/m^2 \cdot day$	0.43	0.93	2.6	KS F4936[24]
Impact resistance	N·m	12.25	12.25	9.8	ASTM D2794[25]
Wear index	mg	141	166	4	ASTM D4060[26]
Pull-off strength [coating/carbon steel]	MPa	0.8	0.7	1.7	ASTM D4541[27]
Pull-off strength [coating/rubber/carbon steel]	MPa	7.8	8.1	18.2	

Table 3 The mechanical properties that were evaluated as excellent for each coating

Coatings	Excellent mechanical properties	
A	1. Flexural modulus 3. Water absorptivity	2.Shore D hardness 4. Impact resistance
B	1. Compressive strength	2.Impact resistance
C	1. Flexural strength 3. Tensile elongation 5. Wear index 6. Pull-off strength [coating/rubber/carbon steel] 7. Pull-off strength [coating/carbon steel]	2. Tensile strength 4. Shore D hardness

the compression test, flexural test, tensile test, surface hardness measurement, water permeation test, impact test, wear test, and pull-off test according to each standard. Each test was performed 3 times and the mechanical properties were averaged. Among the properties, smaller water absorptivity and wear index mean better. Table 3 reveals the mechanical properties for each coating that were evaluated as excellent. The A coating shows excellent flexural modulus, water absorptivity, Shore D hardness, and impact resistance, while B coating shows excellent compressive strength and impact resistance. On the other hand, C coating reveals the seven kinds of excellent properties – flexural strength, tensile strength and tensile elongation, Shore D hardness, wear index, and pull-off strengths.

3.2 Ultrasonic cavitation erosion rate and its failure mechanism of epoxy coatings

[Effect of ultrasonic cavitation time and amplitude on the cavitation erosion rate]; Fig. 3 shows the effect of cavitation time on the cavitation erosion rate of epoxy coatings and carbon steel in 3.5% NaCl at 15 °C. Note that the rate of carbon steel was referred to our recent report reference [10], Fig. 3a was ultrasonically cavitated under the ultrasonic amplitude of 15 μm. As the cavitation time was increased, the cavitation erosion rate increased, regardless of the materials. Its rate of carbon steel was relatively higher than the coatings, but the resistance of C coating was the best. Fig. 3b shows the result under ultrasonic amplitude of 50 μm. As the cavitation time was increased, the cavitation erosion rate increased regardless of the materials, but the cavitation erosion rates of A and B coatings were higher than that of carbon steel and C coating revealed the best resistance. Fig. 3c depicts the cavitation erosion rate under ultrasonic amplitude of 85 μm. B and A coatings revealed very high cavitation erosion rate over 80 mm/y, regardless of the cavitation time. Since these rates were very much higher than that of carbon steel, these mean that A and B coating cannot protect

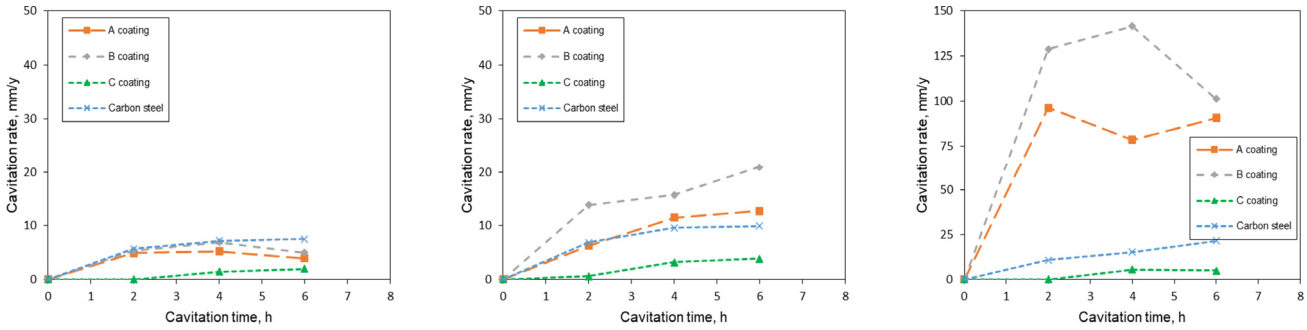

Fig. 3 Effect of cavitation time on the cavitation erosion rate of epoxy coatings and carbon steel in 3.5% NaCl at 15 °C(the rate of carbon steel was referred to the reference [10]); (a) ultrasonic amplitude 15 μm, (b) ultrasonic amplitude 50 μm, and (c) ultrasonic amplitude 85 μm.

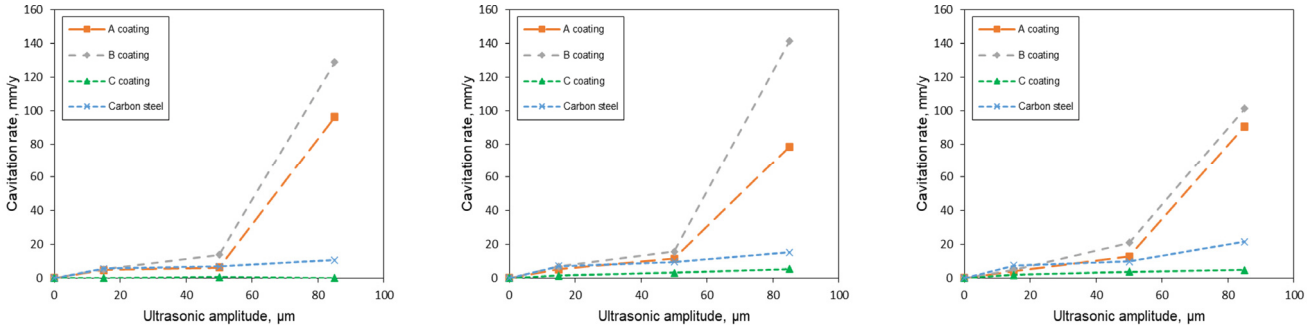

Fig. 4 Effect of ultrasonic amplitude on the cavitation erosion rate of epoxy coatings and carbon steel in 3.5% NaCl at 15 °C(the rate of carbon steel was referred to reference [10]); (a) after 2 h, (b) after 4 h, (c) after 6 h.

the base metal of the pipe in this cavitation condition. However, C coating showed the best cavitation erosion resistance in this condition.

On the other hand, Fig. 4 shows the effect of ultrasonic amplitude on the cavitation erosion rate of epoxy coatings and carbon steel in 3.5% NaCl at 15 °C. The rate of carbon steel was referred to the reference [10]. Regardless of cavitation time, as the ultrasonic cavitation amplitude was increased, the cavitation erosion rates of A and B coatings increased gradually until the amplitude of 50 μm. However, the cavitation erosion rates abruptly increased at amplitude 85 μm. In the case of carbon steel, its rate relatively gradually increased with the amplitude. As described above, C coating revealed the best cavitation resistance.

[Relationship between cavitation rate and mechanical properties]; Fig. 5 compares the relationship between the cavitation resistance of epoxy coatings, and the following properties: (a) compressive strength, (b) flexural strength, (c) flexural modulus, (d) impact resistance, (e) Shore D hardness, (f) water absorptivity, (g) tensile strength, (h) wear index, and (i) pull-off strength for coating/rubber/carbon steel. Cavitation rate was determined at the amplitude of 85 μm for 6 h in 3.5% NaCl at 15 °C as shown in Fig. 3 and 4. Fig. 5a, shows that there is little relationship between the compressive strength and cavitation resistance, because of the very low determination coefficient of 0.0695. Fig. 5b and 5c show there is close relationship between the flexural strength and cavitation resistance, because of the high determination coefficient of 0.7564, unlike flexural modulus. Fig. 5d shows that there is little relationship between impact resistance, and cavitation resistance because higher impact resistant coating revealed high cavitation rate. Fig. 5e shows that there is little relationship between Shore D hardness and cavitation resistance, because of the very low determination coefficient of 0.3408. Fig. 5f shows that there is little relationship between the water absorptivity and cavitation resistance because lower water absorptive coating revealed high cavitation rate. Fig. 5g shows that there is close relationship between tensile strength and cavitation resistance

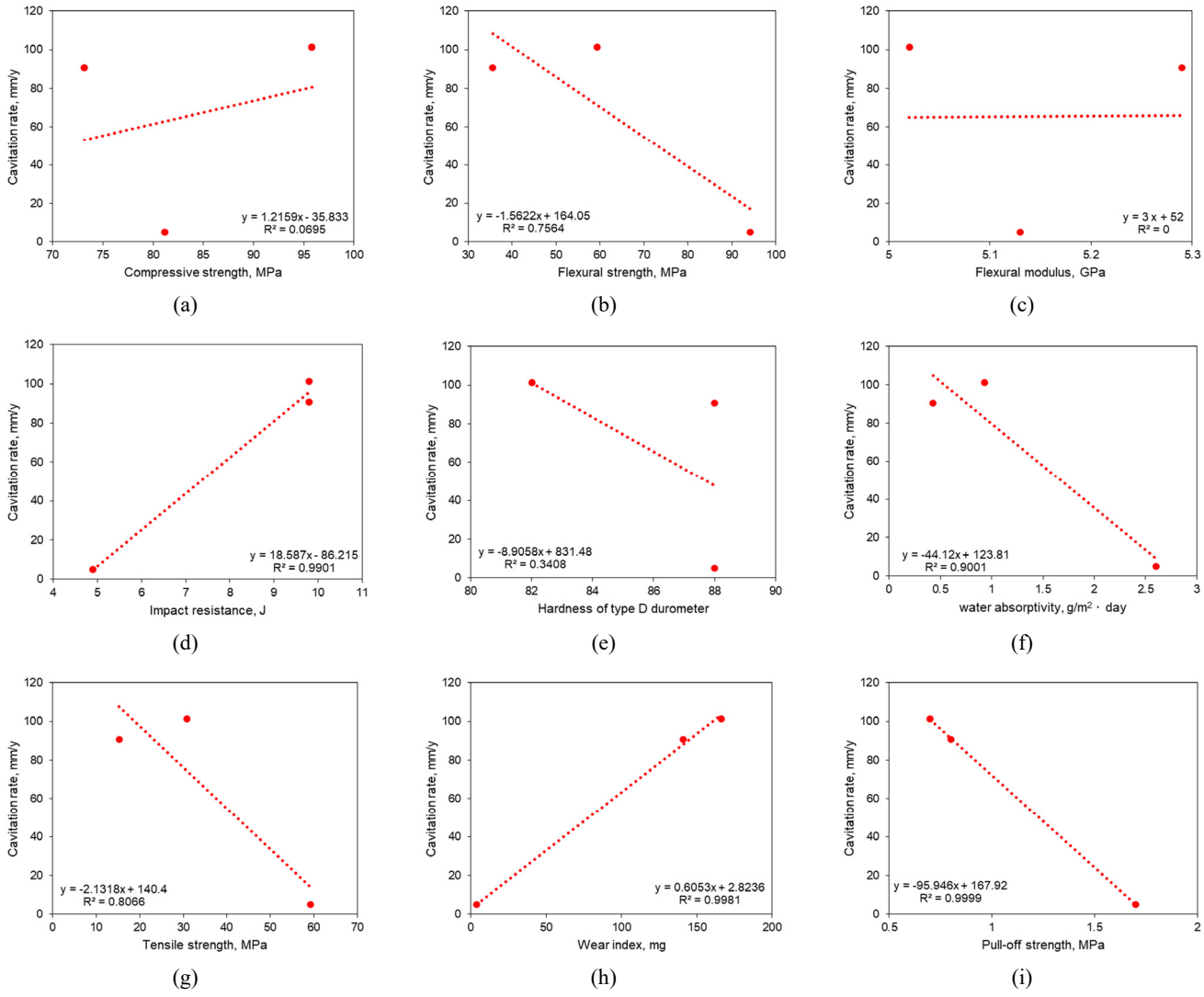

Fig. 5 Relationship between the cavitation resistance(ultrasonic amplitude 85 µm, 6 h) of epoxy coatings and the following properties: (a) compressive strength, (b) flexural strength, (c) flexural modulus, (d) impact resistance, (e) Shore D hardness, (f) water absorptivity, (g) tensile strength, (h) wear index, and (i) pull-off strength[coating/rubber/carbon steel].

because of the high determination coefficient of 0.8066. Fig. 5h shows that there is close relationship between the wear resistance and cavitation resistance, because of the very high determination coefficient of 0.9981. Fig. 5i shows that there is close relationship between the pull-off strength and cavitation resistance, because of the very high determination coefficient of 0.9999. In summary, flexural strength, tensile strength, wear resistance and pull-off strength were closely related to the cavitation resistance of the coating.

In order to compare the cavitation erosion resistance of the coated sample, we prepared the epoxy-coated rubber-lined carbon steel, and performed the cavitation erosion test on the cross section of the specimen. Fig. 6

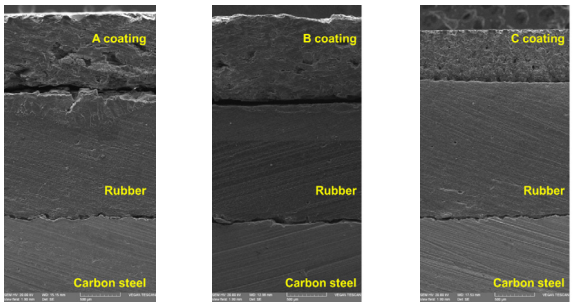

Fig. 6 Appearance of the cross section of coatings/rubber/carbon steel after cavitation erosion test in 3.5% NaCl at 15 °C (Amplitude 85 µm, 2 hours cavitation, SEM, ×200): (a) A coating, (b) B coating, and (c) C coating.

shows the appearance (SEM, ×200) of the cross section of coatings/rubber/carbon steel after cavitation erosion test in 3.5% NaCl at 15 °C. The amplitude was 85 μm and 2 h cavitation was applied. As confirmed in the figures, the coating, and the interface between the coating and rubber, of A and B coatings were severely cavitation-eroded, but the C coating/rubber specimen showed excellent performance.

[Cavitation mechanism of 3 kinds of epoxy coatings]; Fig. 7 shows the surface appearance (digital camera) of a, a', a" A coating, b, b', b" B coating, and c, c', c" C coating after cavitation corrosion test using ultrasonic amplitude of 85 μm in 3.5 % NaCl at 15°C. Fig. 7a, b, c are for 2 h cavitation time, Fig. 7a', b', c' are for 4 h cavitation time, and Fig. 7a", b", c" are for 6 h cavitation time. As the cavitation time was increased, the cavitated surfaces were greatly roughened, and the extent of the damaged area of A and B coatings was severely larger than that of C coating. These trends coincided in the results of Fig. 3 and 4. Fig. 8 reveals the 3D topography of a, a', a" A coating, b, b', b" B coating, and c, c', c" C coating after cavitation corrosion test using ultrasonic amplitude of 85 μm in 3.5 % NaCl at 15 °C. When the cavitation time was 6 h, the maximum depths of damage of the coatings were 1780, 1850 and 800 μm respectively. These trends confirmed the results

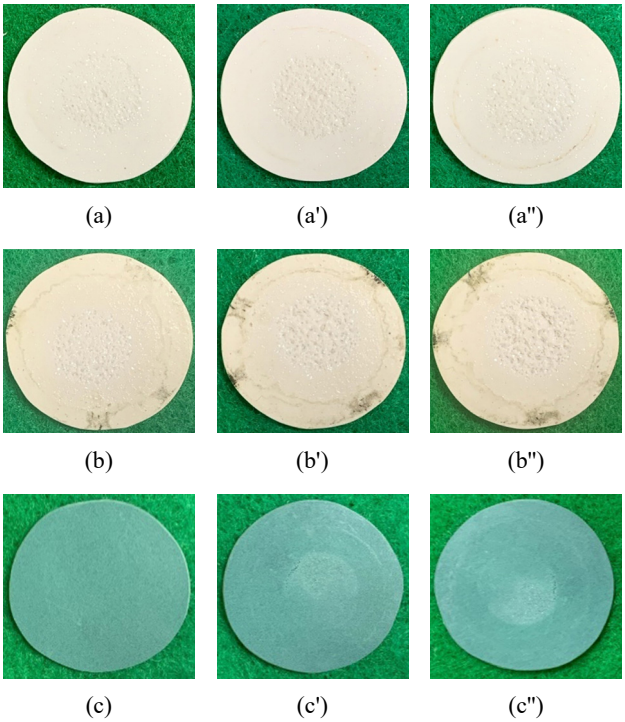

Fig. 7 Surface appearance (digital camera) of (a, a', a") A coating, (b, b', b") B coating, and (c, c', c") C coating after cavitation corrosion test(amplitude : 85 μm) in 3.5 % NaCl at 15 °C: (a), (b), (c) Cavitation time 2 h, (a'), (b'), (c') Cavitation time 4 h, (a"), (b"), (c") Cavitation time 6 h.

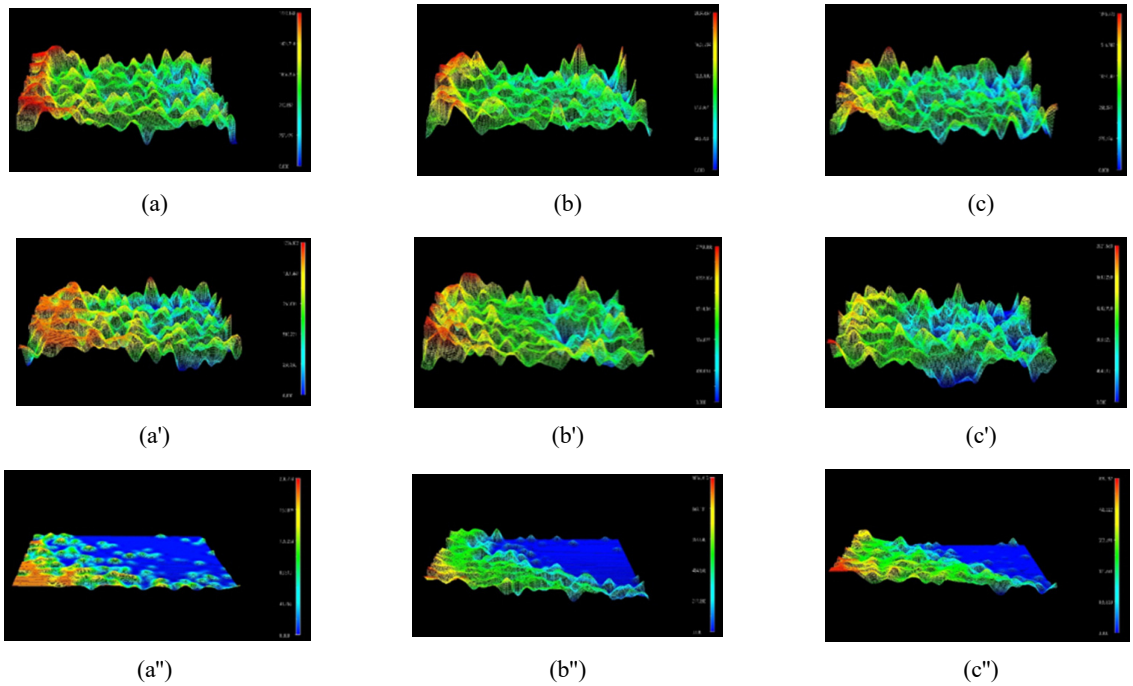

Fig. 8 3D topography of (a, a', a") A coating, (b, b', b") B coating, and (c, c', c") C coating after cavitation corrosion test(amplitude : 85 μm) in 3.5 % NaCl at 15 °C: (a), (b), (c) Cavitation time 2 h, (a'), (b'), (c') Cavitation time 4 h, (a"), (b"), (c") Cavitation time 6 h.

of Fig. 3 and 4.

Fig. 9 depicts a, a' SEM image and the distribution of b, b' carbon, c, c' oxygen, d, d' silicon on the surface, which corresponds to the cavitated area/solution exposed area I(left photos) and the solution exposed area II/specimen hold area(right photos) of A coating after

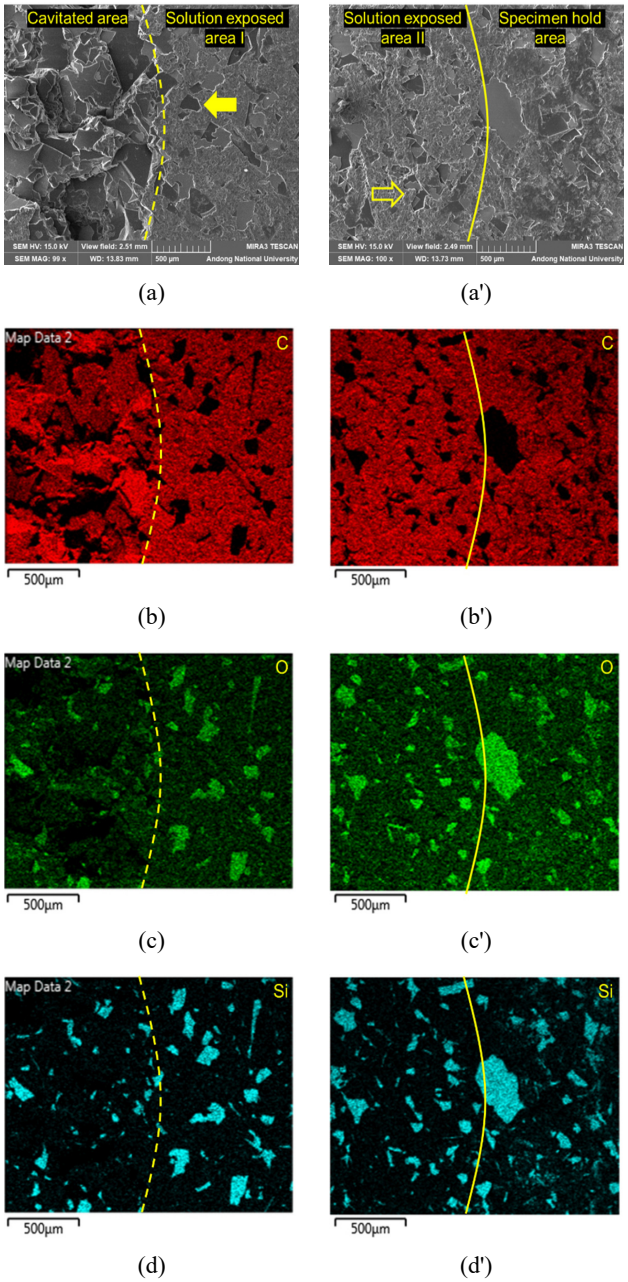

Fig. 9 (a, a') SEM image, (b, b') distribution of carbon, (c, c') distribution of oxygen, (d, d') distribution of silicon on the surface(cavitated area/solution exposed area I/solution exposed area II/specimen hold area) of A coating after cavitation test (amplitude 85 μm, 6 h) in 3.5 % NaCl at 15 °C.

cavitation test using ultrasonic amplitude 85 μm for 6 h in 3.5 % NaCl at 15 °C. In the case of the specimen hold area, the appearance was almost the same as that of the specimen before test. In the case of the solution exposed area II, the compounds of the surface were very slightly damaged (open arrow), because the surface was only exposed to the solution, not cavitated, and the distribution of main elements was almost the same as those of the specimen hold area. In the case of the solution exposed area I, the compounds of the surface were damaged (solid arrow) because the surface was indirectly affected by the cavitation bubbles. In the case of the cavitated area, the matrix and compound were severely damaged and this was proved by the reduction of carbon and oxygen, and the no-detached compound remained and this was also proved by the distribution of silicon.

Fig. 10 reveals a, a' SEM image and the distribution of b, b' carbon, c, c' oxygen, d, d' silicon on the surface of B coating obtained in the same condition as Fig. 9. In the case of the solution exposed area II of Fig. 10a', the surface looks like the resin-flow appearance by the reaction of the coating and the salt water. In the case of the solution exposed area I, the resin-flow surface was a little washed and damaged because of cavitation bubble near the horn tip. In the case of the cavitated area, the matrix was eliminated and then the compounds came to the front and this was proved by the reduction of carbon and the increase of silicon.

Fig. 11 shows a, a' SEM image and the distribution of b, b' carbon, c, c' oxygen, d, d' silicon on the surface of C coating obtained in the same condition as Fig. 9. As described in Fig. 2, the compound has a polygonal shape. In the case of the solution exposed area I, the interface of the matrix and compound was damaged and the compounds were detached because of cavitation bubble near the horn tip. In the case of the cavitated area, the matrix and compound were detached, and the compound that was small and well distributed was newly shown and this is proved by the distribution of silicon.

Based on the observations described above, the cavitation erosion mechanism of epoxy coatings was proposed. Fig. 12 shows the degradation steps of epoxy coatings by ultrasonic cavitation test in 3.5 % NaCl at 15 °C. Step 1 is the immersed stage in a stagnant solution. Step 2 is the initial stage of cavitation erosion and in this stage, the compound or the matrix or the interface of the matrix and compound depending upon the components used in the coatings were partly damaged. Step 3 is the propagation stage and the coating was se-

verely damaged regardless of the matrix and compound. Step 4 is the final stage and the thickness of the coating was reduced and the surface was heavily roughened, and the non-detached compounds remain. High cavitation resistant coating had high compressive strength, tensile strength, pull-off strength, and wear resistance, as described in Fig. 5. These properties could affect the resistance of the initial and propagation stages in cavitation erosion of the coatings, and the small and polygonal shape's compound in C coating was also effective in terms of its resistance.

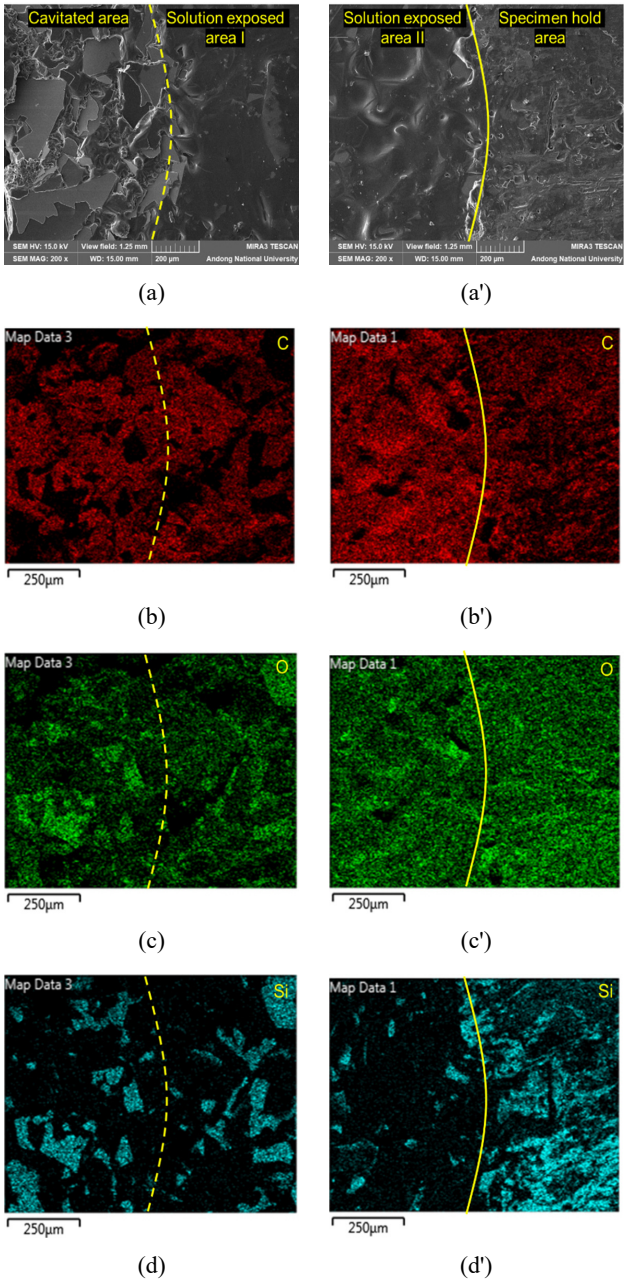

Fig. 10 (a, a') SEM image, (b, b') distribution of carbon, (c, c') distribution of oxygen, (d, d') distribution of silicon on the surface(cavitated area/solution exposed area I/solution exposed area II/specimen hold area) of B coating after cavitation test (amplitude 85 μm, 6 h) in 3.5 % NaCl at 15 °C.

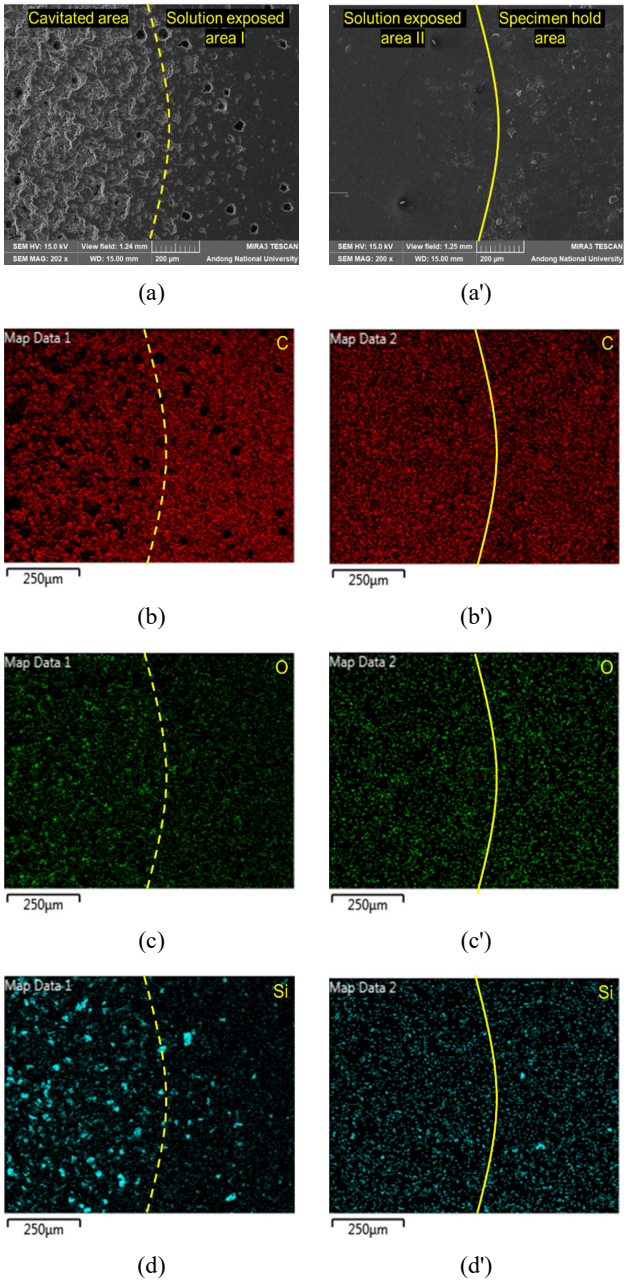

Fig. 11 (a, a') SEM image, (b, b') distribution of carbon, (c, c') distribution of oxygen, (d, d') distribution of silicon on the surface(cavitated area/solution exposed area I/solution exposed area II/specimen hold area) of C coating after cavitation test (amplitude 85 μm, 6 h) in 3.5 % NaCl at 15 °C.

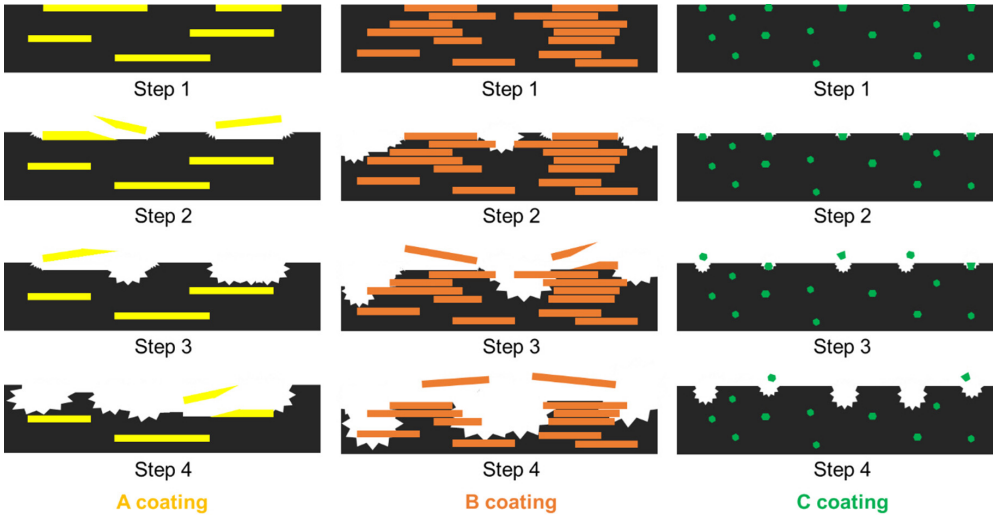

Fig. 12 Degradation steps of epoxy coatings by ultrasonic cavitation test in 3.5 % NaCl at 15 °C : Step 1 (before test), Step 2 (initial stage), Step 3 (propagation stage), Step 4 (final stage).

4. Conclusions

In this work, three kinds of epoxy coatings from three different companies were used, and the cavitation resistance of the coatings was evaluated in 3.5% NaCl at 15 °C using an indirect ultrasonic cavitation method. We found that:

1) The cavitation resistance of the coating was closely related to the flexural strength, tensile strength, wear resistance and pull-off strength of the coating.
2) The cavitation erosion mechanism includes the initial stage and propagation stage; in the initial stage of cavitation erosion, the compound, matrix, or interface of the matrix and compound, depending upon the components used in each coating, were partly damaged. In the propagation stage, the coating was severely damaged regardless of the matrix and compound. High cavitation resistance coating had high flexural strength, tensile strength, pull-off strength, and wear resistance, and thus these properties could affect the resistance of the initial and propagation stages in cavitation erosion of the coatings and a small and polygonal shape's compounds were also effective for its resistance.

Acknowledgments

This work was supported by the KOREA HYDRO & NUCLEAR POWER CO., LTD (No. 2019-Technical-08).

References

1. W. Deng, Y. An, X. Zhao, C. Zhang, L. Tang, and J. Liu, *Surf. Coat. Technol.*, **399**, 126133 (2020). https://doi.org/10.1016/j.surfcoat.2020.126133
2. I. C. Park and S. J. Kim, *Surf. Coat. Technol.*, **376**, 31 (2019). https://doi.org/10.1016/j.surfcoat.2018.08.098
3. I. C. Park and S. J. Kim, *Appl. Surf. Sci.*, **483**, 194 (2019). https://doi.org/10.1016/j.apsusc.2019.03.277
4. I. I. Silveira, A. G. M. Pukasiewicz, D. J. M. Aguiar, A. J. Zara, and S. Bjorklund, *Surf. Coat. Technol.*, **374**, 910-922 (2019). https://doi.org/10.1016/j.surfcoat.2019.06.076
5. H. Sun, *J. Mech. Sci. Technol.*, **26**, 8, 2535 (2012). https://doi.org/10.1007/s12206-012-0633-y
6. D. G. Shchukim, E. Skorb, V. Belova, and H. Mohwald, *Adv. Mater.*, **23**, 1922-1934 (2011). https://doi.org/10.1002/adma.201004494
7. A.Thiruvengadam, *J. Basic Eng.*, **85**, 3, 365 (1963). https://doi.org/10.1115/1.3656610
8. M. S. Plesset and A. T. Ellis, *Mater. Sci.*, **77**, 1055 (1955).
9. B. Vyas and C. M. Preece, *Metall. Trans. A*, **8**, 915 (1977). https://doi.org/10.1007/BF02661573
10. I. J. Jang, K. T. Kim, Y. R. Yoo, and Y. S. Kim, *Corros. Sci. Tech.*, **19**, 163 (2020). https://doi.org/10.14773/cst.2020.19.4.163
11. J. A. Jeong, M. S. Kim, S. D. Yang, C. H. Hong, N. K. Lee and D. H. Lee, *J. Korean Soc. Marine Eng.*,

42, 280 (2018).
https://dx.doi.org/10.5916/jkosme.2018.42.4.280
12. S. Y. Lee, K. H. Lee, C. U. Won, S. Na, Y. G. Yoon, M. H. Lee, Y. H. Kim, K. M. Moon, and J. G. Kim, *J. Ocean Eng. Technol.*, **27**, 79 (2013).
https://dx.doi.org/10.5574/KSOE.2013.27.3.079
13. J. H. Jeong, Y. H. Kim, K. M. Moon, M. H. Lee, and J. G. Kim, *J. Korean Soc. Marine Eng.*, **37**, 877 (2013).
https://dx.doi.org/10.5916/jkosme.2013.37.8.877
14. Y. Huang and D. Ji, *Sensors and Actuators B: Chemical*, **135**, 1, 375 (2008).
https://dx.doi.org/10.1016/j.snb.2008.09.008
15. V. Lefevre, K. Ravi-Chandar, and O. Lopex-Pamies, *Int. J. Fract.*, **192**, 1 (2015).
https://doi.org/10.1007/s10704-014-9982-0
16. F. G. Hammitt, N. R. Bhatt, T. M. Mitchell, N. Orlandea, J. M. Stifel, E. E. Timm, and V. M. Wild, *Liquid Impingement and Cavitation Studies of Erosion Resistance of Rubber-coated materials for B. F. Goodrich*, Report No. UMICH-324490-1-T, The University of Michigan, December (1970).
17. W. Deng, G. Hou, S. Li, J. Han, X. Zhao, X. Liu, Y. An, H. Zhou, and J. Chen, *Ultrasonic – Sonochemistry*, **44**, 115-119 (2018).
https://doi.org/10.1016/j.ultsonch.2018.02.018
18. S. Hattori and T. Itoh, *Wear*, **271**, 1103-1108(2011).
https://doi.org/10.1016/j.wear.2011.05.012
19. K. H. Light and V. Caccese, *Development of a cavitation erosion resistant advanced material system*, Project No. UM-MACH-RPT-01-05, The University of Maine, November (2005).
20. ASTM D695, Standard Test Method for Compressive Properties of Rigid Plastics (2015).
21. ASTM D790, Standard Test Methods for Flexural Properties of Unreinforced and Reinforced Plastics and Electrical Insulating Materials (2017).
22. ASTM D638, Standard Test Method for Tensile Properties of Plastics (2014).
23. ASTM D2240, Standard Test Method for Rubber Property—Durometer Hardness (2015).
24. KS F4936, Coating materials for the protection of concrete, Korean Industrial Standards (2018).
25. ASTM D2794, Standard Test Method for Resistance of Organic Coatings to the Effects of Rapid Deformation (Impact) (2019).
26. ASTM D4060, Abrasion Resistance of Organic Coatings by Taber Abraser (2007).
27. ASTM D4541, Standard Test Method for Pull-Off Strength of Coatings Using Portable Adhesion Testers (2017).
28. ASTM G32, Standard Test Method for Cavitation Erosion Using Vibratory Apparatus (2016).